FUNCTIONALIZATION DEPENDANCE OF CALIX[6]ARENE CONTRAST AND SENSITIVITY TO ELECTRON BEAM EXPOSURE

THESIS

Presented to the Graduate Council
of Texas State University-San Marcos
in Partial Fulfillment
of the Requirements

for the Degree

Master of SCIENCE

by

Daniel M. Ralls

San Marcos, Texas
December 2008

FUNCTIONALIZATION DEPENDANCE OF CALIX[6]ARENE CONTRAST AND SENSITIVITY TO ELECTRON BEAM EXPOSURE

Committee Members Approved:

_____

Gregory Spencer

_____

Michael Blanda

_____

Carl Ventrice

Approved by:

_____

J. Michael Willoughby

Dean of the Graduate College

COPYRIGHT

by

Daniel M. Ralls

2008

ACKNOWLEDGEMENTS

I have to thank my family for their help, from my brother and sisters, step brothers and sister, step mom and dad, and most importantly my Mother and Father. In everything from financial to emotional support my family has helped me through my many years in college.

Dr. Spencer has played a huge role in my life and career at Texas State University-San Marcos. I have learned many things as his student, and many more as his RA. Of all his lessons the most important has been his constant sense of humor. While few physics problems can be solved with a sense of humor, a good one will get you through with less trouble and more friends, a lesson I take to heart. I would like to also mention Dr. Ventrice and Dr. Blanda. They have given me the benefit of their years as researchers and teachers and their guidance has been helpful beyond measure. I owe the entire Department of Physics a great deal, as my five years at Texas State have been my best. I'm extremely thankful to the entire department, faculty and staff both present and former. Dr. Anup Bandyopadhyay has been especially helpful and patient with me through the years. A special thanks to Dr. James R. Crawford; his presence has affected virtually every part of my life at Texas State.

I would also like to thank my friends, both here at Texas State and elsewhere. Those who have helped with my school work, others who have helped with my research, and all that have helped in my life.

TABLE OF CONTENTS

Page

List of Tables

Table **Page**

List of Figures

Figure **Page**

CHAPTER 1

Introduction

With the advent and implementation of modern semiconductor based transistors and integrated circuits (IC) in the 1950's the world saw a vast change in the size and functionality of household electronics. The first devices to see major advancements were radios and televisions, becoming smaller with reduced power consumption and increased capabilities, and all at a lower cost. Improving existing devices, however, was far from the limit of the developing IC field; creative minds continue to find new areas and ways to apply the technology. Simply applying the technology is not enough either; the world demands increasingly powerful and compact devices. While the definition of power depends on the device, anything from signal amplification to computation, the solution is to add more transistors to more efficient IC designs. While the design of the IC plays an important role in both IC size and efficiency, transistor size provides the ultimate limit in both areas. By reducing the size of the transistor the inherent loses due to material resistivity are reduced, thus any transistor or IC design will be more efficient if simply reduced in size. The reduction in size also

allows for more transistors to be placed in the same sized device. A paper published in 1965 by Dr. Gordon Moore, co-founder and former CEO of Intel, outlined the idea that the number of transistors on an integrated circuit should double roughly every two years, commonly called Moore's Law (Figure 1.1).

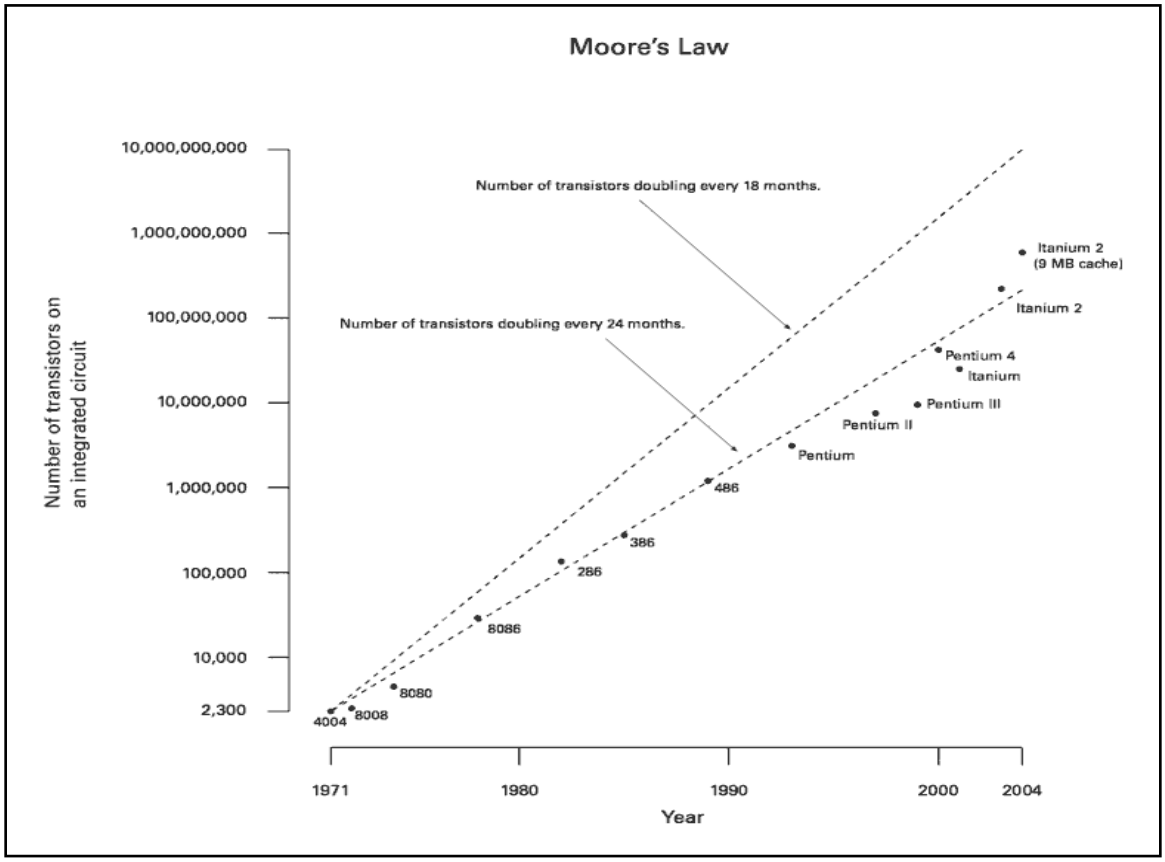

Figure 1.1: Moore's Law. The prediction of the exponential increase of the number of transistors on an integrated circuit. [3]

There is a good argument to be made that Moore's law is a self fulfilling prophecy; that the industry is trying to keep up with its own golden rule. With Dr. Moore at the head of Intel, one of the world's largest IC manufactures of the time, he was certainly in a position to ensure that his prediction was met. This is, however, beside the point. In the last 35 years the standard IC has gone from a combination of two thousand transistors to roughly half a billion, almost exactly

in-line with Moore's Law. Achieving these benchmarks has been done in a variety of ways, but all involve the refinement of IC production through photolithography.

The basis of modern IC production is photolithography, using light-sensitive photoresists that either becomes soluble (positive) or insoluble (negative) to a certain solvent or solvents after exposure to photons of sufficiently high energy. The target wafer, normally a uniformly doped silicon wafer, is covered with the resist. A photomask is placed on or just above the wafer, covering, with opaque features, portions of the wafer to prevent them from being exposed while the transparent portions of the mask permits the uncovered regions to be exposed. After exposure the wafer is put through a development process in which solvents remove the soluble portion of the resist coating. This allows a production process to be performed on either the exposed or unexposed regions, for positive or negative resists respectively, while protecting the other portions of the wafer. When first considered, the limitation may seem to be the quality and precision of the photomask and production process as a whole. This and other limitations come into play.

The other main limitation of photolithography is the wavelength of the light used. In modern photolithographic processes 193 nanometer (nm) light is used in many applications.[5] This was not an issue until the late nineties when microfabrication process approached the 200 nm barrier. Since then the microfabrication industry has developed several techniques to decrease to feature size below that of the wavelength of light used, however these techniques fall outside the scope of this paper. These rather innovative techniques along with the advent of advanced materials (such as high-k dielectrics) have carried the

industry to the 45 nm benchmark in current production microprocessors. With the increased resolution needed the door for electron beam lithography has been opened.

1.1 Electron Beam Lithography

Electron beam lithography has many advantages which can be utilized by modern microfabrication processes. The main advantage is the size, or more precisely the wavelength, of a single energetic electron. This wavelength may be found by using Dr. Louis de Broglie's equation for the wavelength of an electron.

$$\lambda_e = \frac{h}{\sqrt{2m_e eU}} \qquad (1.1)$$

Here λ_e is the wavelength of an electron accelerated by a voltage U, h Planck's constant, m_e is the rest mass of an electron, and e is the fundamental charge. The possible accelerating potentials in an electron microscope can range from less than a kilovolt (kV) to higher than 30 kV. The accelerating voltage used in this study is 20 kV which gives an electron wavelength on the order of ten picometers (pm), far smaller than a hydrogen atom. This is well beyond the limit necessary for any lithographic process, which is an advantage over light in that no special tricks are needed to produce structures smaller than the wavelength used.

Electron beams can also be directed by electric and magnetic fields. This is commonly seen in Electron Microscopes which can adjust the beam parameters to focus the beam on a specific area and raster the beam to scan

different areas. In such systems the resolution is limited to the beam spot size produced, which can be less than 1nm[1]. Such a system could be used to systematically expose a sample in a preset pattern.

Electron beam lithography has been used in the semiconductor industry for several decades, using a wide variety of resists. One of the more commonly used resists is Poly(methyl methacrylate) (PMMA), having a very high resolution though at the cost of being less sensitive than other resists.[4]

With current equipment this process is too time consuming to use as a mass production technique, but it is an attractive technique for rapid prototyping and research as it avoids the need for photomasks which can add greatly to project costs. For mass production it could be possible to use masks in conjunction with a broad beam electron source, but with current technology it would likely be less efficient in both cost and time than current photolithography techniques.

The most likely commercial use for electron beam lithography is in photomask production. Photomasks being the core of photolithography, a production process is only as good as the masks used. When a company produces an IC for commercial use or sale it's normally done on a very large wafer, such that hundreds or thousands of circuits are produced per wafer. So the precision and accuracy of a photomask is paramount, as it must not merely reproduce the features designed by the engineers but every design on the mask must line up with dozens of other masks with nanometer tolerances. With computer controlled beam patterning for accuracy and precision in the nanometer range electron beam lithography is a logical choice.

CHAPTER 2

Chemistry of Calix[6]arenes

Calixarenes, a class of organic molecule, are composed of specific structural units, called benzene rings, arranged in a macrocyclic ring. Benzene is an aromatic hydrocarbon, abbreviated as arene. Calix is derived from the Latin word for cup due to the molecule's cup shape, as seen bellow in Figure 2.1. The number of benzenes in the macrocycle denotes the different sizes of calixarenes, the particular calixarene in this study has six benzene rings, giving a diameter of roughly 1nm and the name calix[6]arene. Other calix[n]arenes, where n is the number of benzenes in the macrocycle, may be formed.[8]

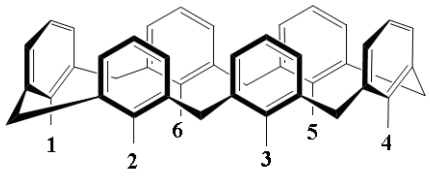

Figure 2.1: The calix[6]arene base molecule.[2]

Calix[4]arenes have been studied extensively, showing a higher resolution and better etch rates than PMMA but with a lower sensitivity, depending upon the functional groups attached.[9] The upper and lower rims of the calixarene annulus can be modified by attaching functional groups. By selectively functionalizing the

calixarene it can be tailored to suit a specific need, whether that be increased sensitivity, an improved etch rate, or some more specific need. It is this synthetic versatility that has led to the number of studies featuring different calix[n]arenes and their applications in supramolecular chemistry.[5-7]

One reason the calix[4]arene was originally chosen over the calix[6]arene because of the increased difficulty of synthesizing the calix[6]arenes. However recent work has mitigated some of these difficulties, and with the increased number of benzene rings it can be further functionalized. Through this increased functionalization it is hoped to increase the sensitivity of the calix[6]arene to beyond that of PMMA while retaining the high resolution and low etch rates of other calixarenes.

The calix[6]arene may be conformationally locked into one or two conformations. Xylenyl groups, composed of a single benzene ring, are bonded between two of the benzene rings in the calix[6]arene macrocycle. Hexyl groups, which are composed of a chain of six carbon atoms with thirteen hydrogen atoms completing the molecular structure, are attached to the calix[6]arene at two locations prior to the attachment of the xylenyl groups. The hexyl groups are placeholders to prevent the xylenyl groups from bonding at those locations, ensuring that the xylenyl groups bridge the calix[6]arene across the annulus. This is also where the size of the calix[6]arene is defined, the distance across the upper rim of the calix[6]arene, between the two benzene rings functionalized by hexyl groups, is 1nm.

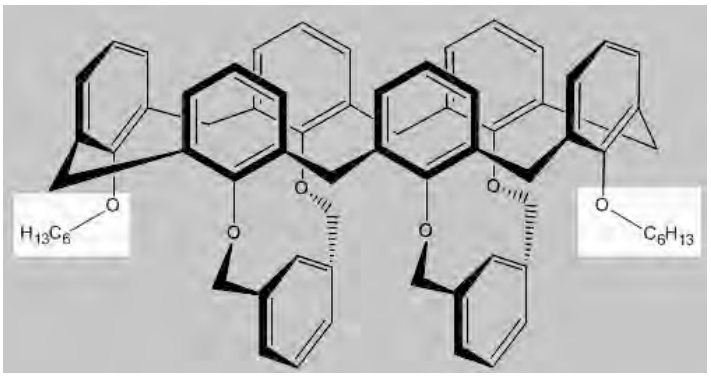

Figure 2.2: The hexyl groups. Placed at both ends to ensure that the addition of functional groups occurs at the proper bonding sites.[2]

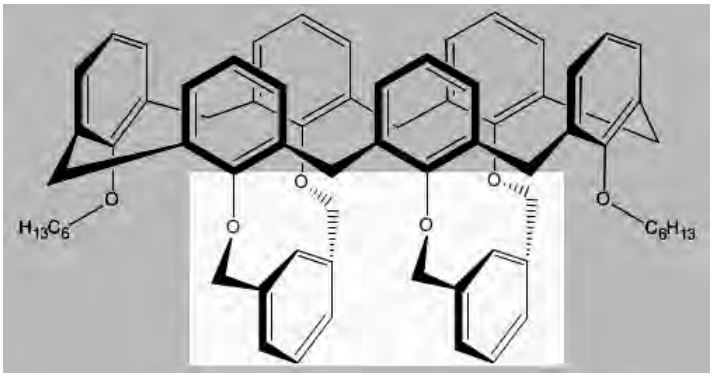

Figure 2.3: The xylenyl groups. Bonded across the molecule to bridge the ring and prevent geometric changes.[2]

The bridging of the ring by the xylenyl groups allows for two of the shapes that the calyx[6]arene may form, these shapes are called conformations and the calix[6]arene is then said to be conformationally locked. The two shapes of study are known as the cone isomer and the 1-2-3-alternate isomer, as seen in Figure 2.4.

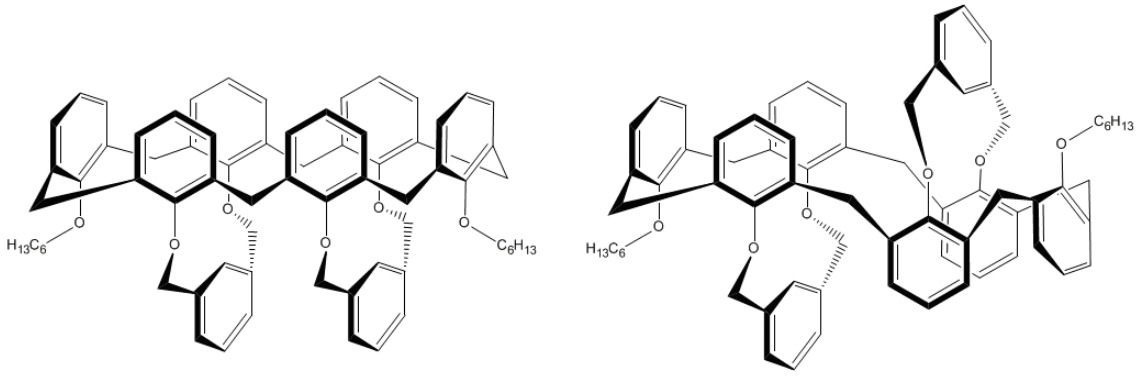

Figure 2.4: Cone (left) and 1-2-3-alternate (right) Conformations.[2]

The xylenyl groups prevent the calix[6]arene from rotating about the carbon bonds joining the benzene rings, thereby prohibiting a shape change. The cone is so called because of its conical shape, and the 1-2-3-alternate because after every third benzene ring the orientation flips. By preventing the calixarene from making conformational changes the chemical and physical properties are prevented from varying. During synthesis both conformations are produced, however the reaction conditions can be modified to favor either conformation and selective crystallization can remove the remainder of the unwanted compound through filtration.

Either conformation can be synthesized with up to eight additional functional groups. In this study the two conformations are modified by varying degrees of functionalization by photopolymerizable allyl groups. Allyl groups are a chain of three carbon atoms with the addition of 5 hydrogen atoms to balance the molecule. The allyl group aids in the polymerization of the calix[6]arene by a high energy source, such as the electron beam in this study.

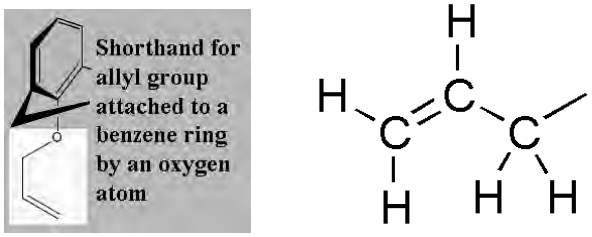

Figure 2.5: Shorthand (left) and the chemical structure (right) of an Allyl Group. Note the double bond between the last two carbon atoms.[2]

For either conformation you can have zero allyl groups, which is un-functionalized, two or four allyl groups, partially functionalized, or six or eight allyl groups, fully functionalized. This gives ten possible compounds between the two conformations. The degree of functionalization refers to the number allyl groups per calix[6]arene molecule. The specific conformation and functionality of the calix[6]arene is referred to first by the number of allyl groups and then by the first letter of the conformation, thus the cone conformation with zero allyl groups is 0C and the 1-2-3-alternate conformation with zero allyl groups is 0A. Below are the chemical shorthand of the different structures that are to be studied.

The purpose of adding the allyl groups is to aid in polymerization of the calix[6]arenes. It has been found that nonfunctionalized calixarenes will polymerize at an increased level of exposure, but that the addition of allyl groups greatly aids the sensitivity and contrast of the calixarene. As stated, the calix[6]arene is being studied as a potential electron beam resist, and two of the major areas of concern are the rate of polymerization, or contrast, and the minimum exposure needed to fully polymerize the film, or sensitivity. The allyl groups are thought to aid in these areas by adding bonds to which other calix[6]arenes, with free radicals, can attach. As shown in Figure 2.5, the allyl

group has two carbon atoms bonded by a double bond. A high energy source, such as an electron beam, can break this double bond.

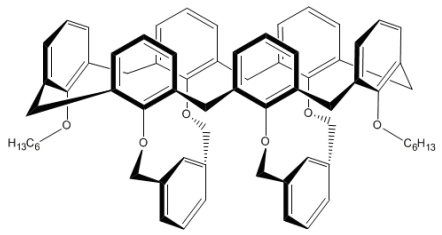

Figure 2.6a: 0C Calix[6]arene

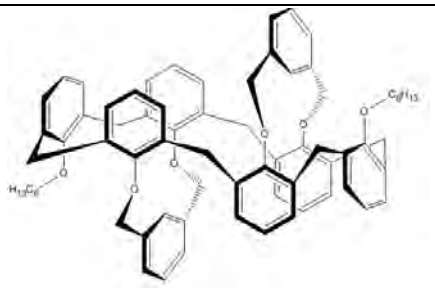

Figure 2.6b: The 0A Calix[6]arene

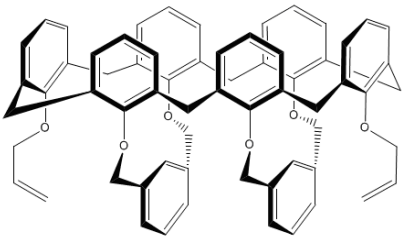

Figure 2.6c: The 2C Calix[6]arene

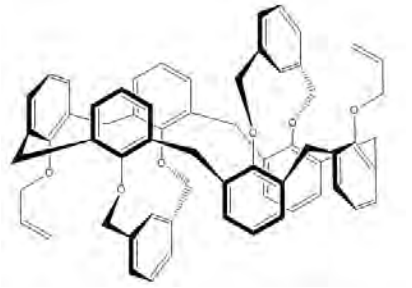

Figure 2.6d: The 2A Calix[6]arene

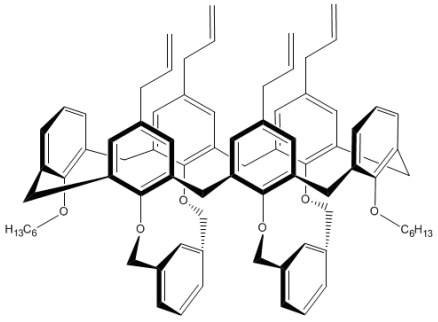

Figure 2.6e: The 4C Calix[6]arene

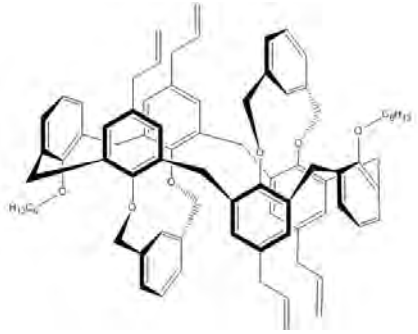

Figure 2.6f: The 4A Calix[6]arene

Figure 2.6(a-f): The ten calix[6]arene molecules of study. Listed by conformation, cone left and 1-2-3-alternate right, and by functionalization from top to bottom.[2]

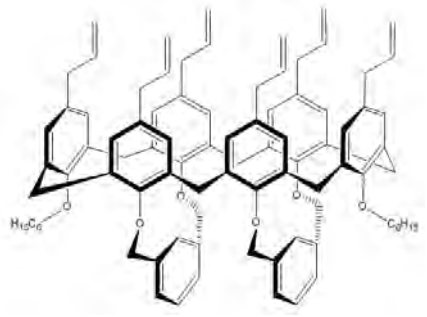

Figure 2.7a: The 6C Calix[6]arene

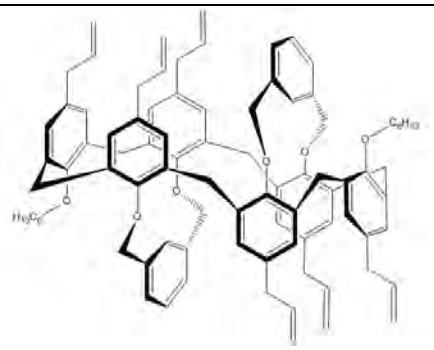

Figure 2.7b: The 6A Calix[6]arene

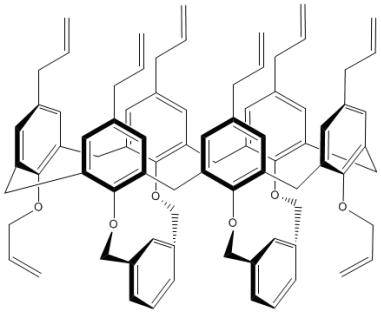

Figure 2.7c: The 8C Calix[6]arene

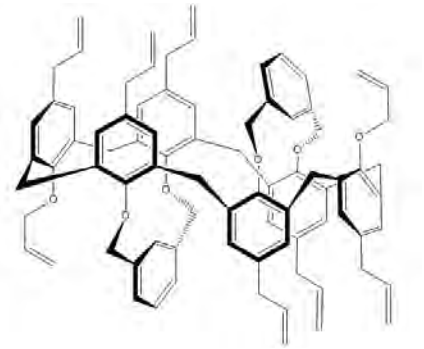

Figure 2.7d: The 8A Calix[6]arene

Figure 2.7(a-d): The ten calix[6]arene molecules of study continued. Listed by conformation, cone left and 1-2-3-alternate right, and by functionalization from top to bottom.[2]

Once the bond is broken one of two things will happen. The bond can reform between the same two carbon atoms, resulting in a non-productive step, or the bond will link to another carbon atom outside of the original allyl group. The latter has two possibilities, either it can bond with another allyl group on the same calix[6]arene, intramolecular bonding, or it can bond with an allyl group on another molecule, intermolecular bonding which is also known as cross-linking or polymerization. Polymerization gives the resultant polymer a much higher resistance to solvents or other possible process that it may be subjected to.

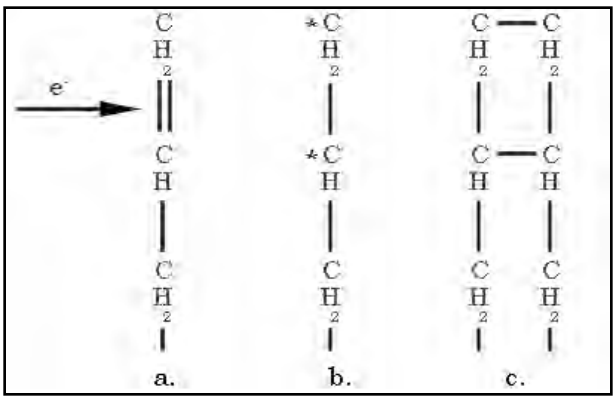

Figure 2.8: The process of cross-linking of allyl groups. a) An electron strikes the allyl group, imparting sufficient energy to break one of the carbon double bonds. b) The broken double bond gives each carbon atom a free radical capable of forming a new bond with another carbon atom. c) The allyl group bonds with another allyl group with a broken double bond.[2]

The mechanics of exposure are not entirely known, but there are a few key facets. The penetration depth of an electron at a 20kV acceleration voltage is greater than the film thickness, so the calix[6]arene film is likely exposed evenly throughout, not top to bottom or bottom to top. This means that there is some statistical probability of an electron striking an allyl group and then some further probability of that allyl group creating an intermolecular bond. The distribution of the exposed and polymerized calix[6]arene film should be essentially random, creating a honeycomb web of polymerized film. It is important to note here that the statistical probability of the entire exposed region being polymerized is likely small. As the incident electrons break the allyl groups they also break intermolecular bonds, causing parts of the film to depolymerize. This will eventually come to a state of equilibrium with some statistical portion of the film being polymerized and some statistical portion being calix[6]arene monomers. The way the polymerized web forms is likely highly dependent on the

conformation and functionalization of the calix[6]arene, producing a different sensitivity and contrast for each. As the functionalization is increased it is expected that the sensitivity should also increase, as there are more allyl groups to create inter-molecular bonds. At the same time it is thought that that the extra bonds may create conditions in which the contrast may suffer, possibly due to excessive bonding between already bonded calix[6]arene molecule.

CHAPTER 3

Procedure

The procedure followed had several major steps including; the deposition of a calix[6]arene film from a solution onto a silicon wafer and the measurement of the film thickness, electron beam exposure and subsequent development of the film, and then imaging of exposed regions with Atomic Force Microscopy (AFM) for analysis.

3.1 Film Deposition and Film Thickness Measurement

To study the calix[6]arenes they need be applied to a test wafer, which is done as it would be for a standard photoresist. The calix[6]arenes at standard temperature and pressure (STP) are solid so to apply them they need be dissolved in a suitable solvent, the most suitable being an organic solvent. Chlorobenzene has several desirable physical properties, including desirable melting and boiling points, but it can also support up to about a 20% concentration of calix[6]arenes before the calix[6]arenes becomes insoluble.[2] It is also a very well understood compound, which is desirable as it eliminates many possible unknown factors. The formulas, as made by Dr. Blanda's research

group, are 1% by weight of calix[6]arene powder dissolved in chlorobenzene. This percentage is sufficient to study the calix[6]arenes, giving film thicknesses of around twenty nanometers depending on the spin coating parameters. A higher percentage can be used but this was deemed sufficient as to not waste the calix[6]arenes, the compounds being somewhat difficult and time consuming to synthesize.

The application of the calix[6]arene solution was done using a substrate spinner to spin on the calix[6]arene solution, see Figure 3.1.

Figure 3.1: Wafer spinner and control panel.

Spinning allows for the even distribution of a thin film from a liquid solution. Using a three step spin program the wafer was spun up to 1000 rpm in 5

seconds, then to 3000 rpm for 30 seconds, and then down to 0 rpm in 5 seconds. Once the spinner had reached 3000 rpm, about 1 second after transitioning from 1000 rpm, three milliliters of the calix[6]arene solution was applied to the spinning wafer. Prior to the application of the calix[6]arene, the wafer is cleaned by first rinsing in acetone and then in isopropyl alcohol, this is done while the wafer is spinning at 3000 rpm. A second spin cycle is done to ensure the wafer is dry. The calix[6]arene solution is drawn into a syringe through a 0.45 μm filter, the filter removes any solid contaminates in the solution to prevent contamination and uneven film distribution. After the program finishes, the wafer is removed and placed on a hot plate at 100°C for one minute, this evaporates the chlorobenzene leaving the calix[6]arene as a thin film. This leaves a film thickness of twenty to thirty nanometers, which is adequate for this study. If thicker films are desired the spinner can be slowed or the calix[6]arene concentration can be increased as this will increase the viscosity of the solution. At this point the wafer is coated and ready for film thickness measurements.

Film thickness is measured using a Gaertner L117 null ellipsometer, shown in Figure 3.2. A null ellipsometer uses a laser to test the optical properties of thin films, including film thickness. It works on the principle that light reflecting off a surface will undergo a phase and amplitude changes, that can be measured with the ellipsometer's linear polarizers.

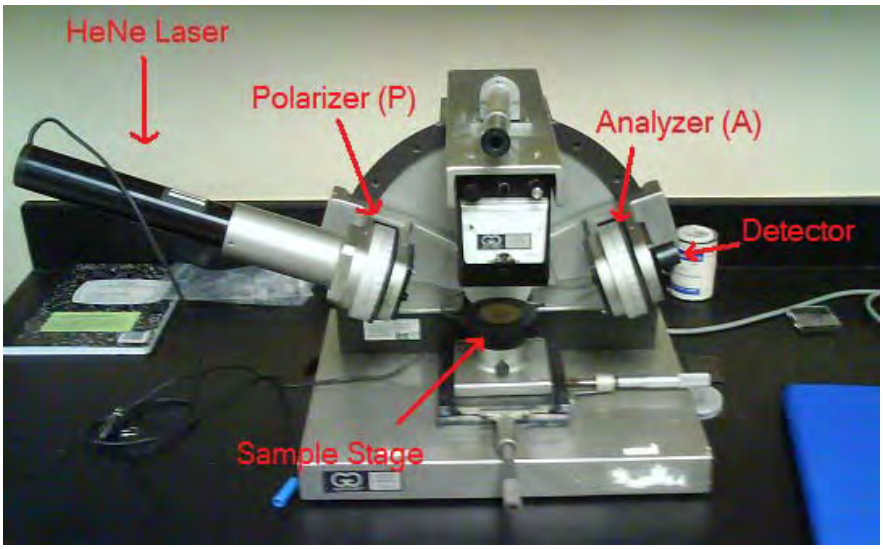

Firgure 3.2: Gaertner L117 null ellipsometer.

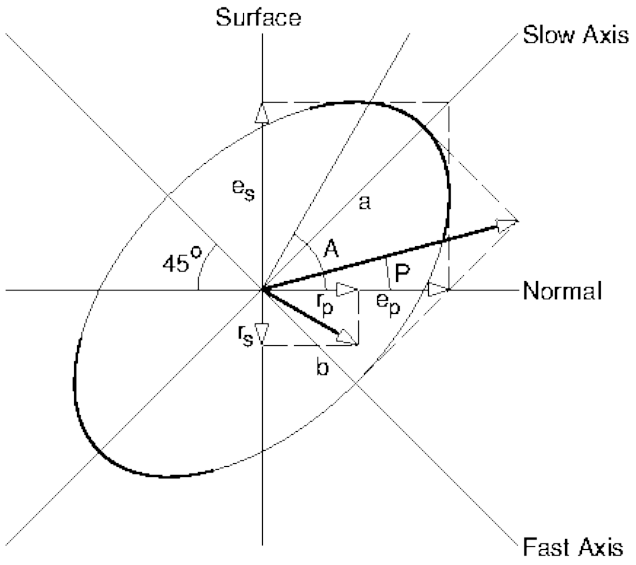

Figure 3.3: Light as it passes through a null ellipsometer.

A 632.8nm helium neon (HeNe) laser creates light which first travels through the polarizer. The polarizer is a polarizing filter set at an angle P to the plane of incidence, shown in Figure 3.3 as Normal. The linearly polarized light

produced is then broken into two components by a quarter wave plate, immediately following the polarizer. The two components are separated by 90 degrees, labeled as fast and slow axes in Figure 3.3. In Figure 3.3 the axis of incidence is the x-axis, and the angle P is the angle the polarizer makes to this axis. The quarter wave plate adjusts the fast and slow axis to -45 and +45 degrees, respectively, away from the normal axis. When the polarizer angle, P, changes it adjusts the relative magnitudes of the fast and slow axis. This changes the shape, or ellipticity, of the emerging beam. The quarter wave plate also retards the slow axis, causing the slow axis to lag behind the fast axis and become out of phase. This is why they are called fast and slow.

As the beam strikes and reflects off the surface the components perpendicular and parallel to the plane of incidence, e_s and e_p respectively in Figure 3.3, are attenuated but to differing degrees depending on the film being measured. The ratio of their attenuation is as follows.

$$\rho = \frac{r_p/e_p}{r_s/e_s} = \tan(\psi)\, e^{i\Delta} \qquad 3.1$$

where r_p and r_s are the respective reflection coefficients. Along with being attenuated, given by the parameter ψ, the two components undergo a phase shift given by the parameter Δ. This adjustment of phase and amplitude of the two components further affects the ellipticity of the light. If adjusted properly, the orientation of the polarizer to the quarter wave plate will produce elliptically polarized light that is the exact opposite of the effect the film has on the light. In

this case, once the light reflects off of the thin film it is transformed from elliptically polarized light back to linearly polarized light. This linearly polarized light travels through another polarizing filter, called the analyzer in Figure 3.2. Since the reflected light is linearly polarized, the analyzer can be rotated to an angle A to nearly completely extinguish the beam such that the reading from the detector is minimized. This is the null position of the ellipsometer, and it is these angles that provide the thin film information.

In use the null ellipsometer is relatively simple. The laser requires a fifteen minute warm up time to ensure consistent results, as the HeNe laser requires some time to warm up to stabilize at full intensity. Once the laser is warm the sample is placed on the stage and the stage height is adjusted to ensure that the reflected laser light is centered in the detector aperture. There are two segments on the dial of each the polarizer and the analyzer. One is in red numbering, 0-90° for the analyzer and 315-135° on the polarizer, and the other segments are numbered in black.

The first objective is to locate the null (or minimum) reading in the red segments. The detector readout reads from 0 to 300, and is most sensitive around 100. There is a gain knob to adjust the amplitude of the signal sent to the readout. In alternating turns the polarizer and analyzer are adjusted to search for the null location, increasing the gain knob to keep the readout around 100 until the gain is increased to its maximum. Once the minimum signal position is located, both the polarizer and analyzer positions are recorded, giving the P_1 and A_1 values. After the gain knob is turned down the polarizer and analyzer can be adjusted to find the second null position. Adding 90° to the original polarizer

reading (so that $P_2 \approx P_1 + 90°$) and subtracting the original analyzer reading from 180° (so that $A_2 \approx 180° - A_1$) will get close to the second null position. Repeating the procedure at these locations finds the second null position, and P_2 and A_2. The values of Δ and ψ can now be calculated.

$$\Delta = 360 - P_1 + P_2 \qquad 3.2 \qquad \psi = \frac{180-(A_1-A_2)}{2} \qquad 3.3$$

here the 1 and 2 refer to the reading in the red and black respectively, and P and A refer to the polarizer and analyzer respectively. The Gaertner L117 null ellipsometer comes with a program for data analysis, Film Wizard 32. The parameters Δ and ψ can be entered into the program and then the desired film properties can be computed. It is important to note that there is a native silicon dioxide (SiO_2) thin film on top of the silicon wafer. The SiO_2 film thickness must first be found to be able to accurately calculate the calix[6]arene film thickness. This was performed at the same time as the calix[6]arene measurement.

The calix[6]arene coated wafer was cleaved into smaller samples to acquire a sample that had a uniform film on it. The spin process is not entirely even and it requires some care to create a wafer with a sufficiently large area to study. The SiO_2 thickness measurement is left to this point as there is some variation of the oxide thickness across the wafer, and in an attempt to gain the most accurate measurement possible an oxide sample adjacent to the calix[6]arene sample is used to test for the oxide thickness. This adjacent sample is stripped of the calix[6]arene film by sonicating in acetone for five minutes, then

in isopropyl alcohol for five minutes and is dried with compressed nitrogen. Afterwards the oxide sample is tested using the ellipsometer. The properties of silicon and SiO_2 are sufficiently well known as to aid in the process. Once the oxide thickness is known, the calix[6]arene film is tested and its thickness and index of refraction are found. While the index of refraction is not the focus of this study, it is required for accurate film thickness measurement.

3.2 Exposure and Development of the Calix[6]arene Film

The calix[6]arene films are exposed using a scanning electron microscope (SEM). The SEM used is a JEOL JSM-6400F high resolution field emission scanning electron microscope using the JEOL Orion control software, see Figure 3.4.

Figure 3.4: JEOL JSM-6400F Scanning Electron Microscope.

The basic layout of SEM starts with the electron gun. This normally consists of an electron source, a filament of some kind not unlike a light bulb filament, and a pair of accelerating grids. These grids have a potential placed across them such that the electrons from the filament are accelerated down towards the sample. The potential across the grids dictates the kinetic energy imparted to the electrons, if the potential is 20kV then the electrons will be given 20keV of kinetic energy. The electrons pass next through the condenser lens; an electromagnetic lens that tightens the electron beam and focuses it towards the aperture. Here the beam must be centered on the aperture, a simple metal plate with a small opening in the center used to reduce background noise from stray electrons. In this study the largest aperture was used to produce the highest beam current. Next is the objective lens. Larger than the condenser, this lens is used to reduce to beam size further for scanning. Depending on the equipment the beam width can be less than 1nm.[1] Last, before the sample itself, are the scanning coils, these coils direct the beam across the sample. This can be done by simply rastering the beam across the sample, as is done in scanning mode, or by an automated patterning which is common in electron beam lithography.

Since the sensitivity of the different calix[6]arene samples are unknown, a small portion of the larger calix[6]arene sample is cleaved for exposure. It is important to have enough samples for several runs, as it is likely to take several attempts to create a sample capable of producing an accurate contrast curve. The cleaved sample is placed on the sample puck, attached using double-sided carbon tape. Carbon tape is used in high vacuum situations as other forms of adhesives will outgas. For visual reference, both in the SEM and later in finding

the exposures, the test sample is scratched with a diamond scribe. The sample chuck is placed in the sample holder and loaded into the load lock. Once the load lock is pumped down, the chamber door can be opened and the sample loaded. After the sample is loaded the chamber door is closed and the chamber is allowed to pump down for several minutes.

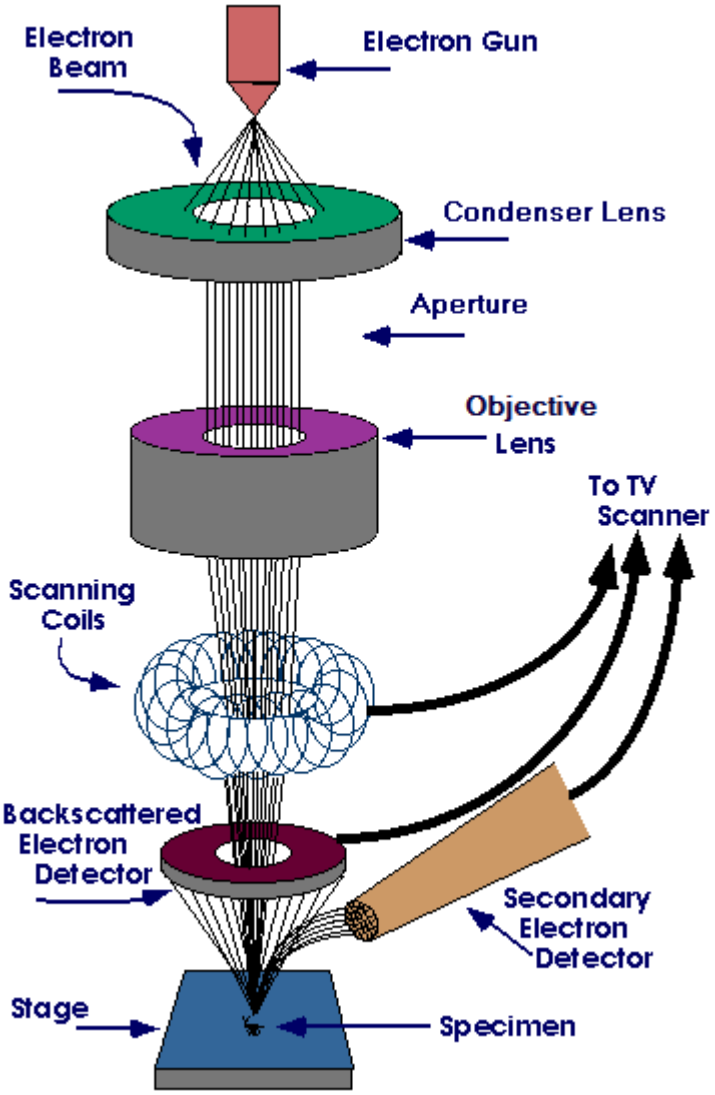

Figure 3.5: Diagram of a Scanning Electron Microscope.

The chamber must reach a base pressure of $2x10^{-6}$ Torr before the electron beam is powered, as excessively high pressure may damage the instrument. The high tension voltage can be turned on once the base pressure is reached; it takes several minutes for the probe current to build.

With the microscope powered up, the parameters can be set for the exposures. For all exposures the aperture in the SEM was set to 1, this is the largest aperture which allows an increased number of electrons through producing a higher beam current. The condenser lens was set to 1, its highest setting which reduces the beam size, also increasing the beam current. An acceleration voltage of 20kV was used throughout the experiments. This is the voltage between the two acceleration grids that accelerate the electrons from the filament to the sample, so each electron has a kinetic energy of 20keV. It should be noted here that the energy needed to break the double carbon bond in the calix[6]arene is roughly 7eV, so the electrons emitted by the SEM should be capable of breaking thousands of these bonds or producing secondary electrons. The question of the kinematics of the electrons path as it travels through the calix[6]arene film and comes in contact with the silicon substrate is quite complex. If the electron reflects off of the substrate and travels back through the film the number of broken bonds will increase significantly. However, if the electron is to highly energetic when it strikes the surface it may drive into the substrate where it may become trapped. There is likely a relationship between exposure time and acceleration voltage but it should effect each of the differently functionalized calix[6]arenes equally and should not affect the comparisons between the differently functionalized calix[6]arenes, the aim of this study.

Once the microscope is powered up and the exposure parameters are set, the scratch is located on the sample and brought into focus. One might ask if it is okay to scan over the sample at low magnification, as the SEM is sending out high energy electrons that are breaking double carbon bonds in the calix[6]arene film. Since the rate of exposure is proportional to the number of electrons per unit area that strike the film, the magnification has a direct influence on exposure time. Most exposures were done at magnifications of either 1,000x or 2,000x and full exposure did not occur until one to three minutes depending on the beam current and calix[6]arene functionalization. At a magnification of 20x, the lowest possible and what was used to place the exposures, the scanned is 50 times larger per side than 1k magnification and has 2500 times the area. Since the exposure time is proportional to the area of the exposure, a film that requires one minute to be exposed at 1k magnification would take roughly 42 hours to expose at 20x, thus any time spent at 20x has a negligible effect on the sample.

Having located the scratch and focused the microscope on the sample the sample can be exposed. Just before the first exposure the probe current detector (PCD) is moved into the beam path, this gives the starting beam current which is necessary for accurately determining the sensitivity and contrast of the sample. This is repeated after about every 5 minutes of microscope use; the microscope is set to keep the emission current at a constant 12μA which causes the beam current to slowly increase. To produce an accurate contrast curve one must make many exposures to accurately trace the film thickness as the exposure time increases. Because of this any given sample may have as many as 40 exposures on it. First the general area of sensitivity would be tested, exposing any given

sample at 5 seconds, 10 seconds, 30 seconds, 1 minute, 2 minutes, 3 minutes, 5 minutes, 7 minutes, 10 minutes and 15 minutes. This would be done at 1k magnification first, and if the exposure time for full polymerization was over 5 minutes the magnification would be increased to 2k to reduce the exposure time. Once the test sample is developed and the sensitivity is found, the full exposure run can be done. Depending on the sensitivity the exposures will be made in either 5 or 10 second intervals, the rate is chosen by the sensitivity as to give at least 12 exposures before full polymerization. If a sample is fully polymerized by 90 seconds than a 5 second interval is used, going from 5 seconds to 3 minutes, 36 total exposures, to ensure the contrast curve is complete. If a sample takes longer to fully polymerize, 3 minutes for example, than a 10 second interval is used through 5 minutes, giving 30 exposures.

After the exposure the sample is developed. The development process relies on the polymerized calix[6]arene film being more resistant to solvents than the calix[6]arene monomers. Xylene, an organic solvent, was used for developing, although isopropyl alcohol and other solvents are suitable for the process as well. The development process differs between the differently functionalized calix[6]arenes. In practice the higher functionalized groups appeared to be more resistant to the xylene development than the lower functionalized groups, needing longer development times to become fully developed. During development the sample is immersed in xylene and gently stirred for 8 to 15 seconds, depending on the functionalization. Afterwards the sample is blown dry with compressed nitrogen and then placed on a hot plate at 105°C for 1 minute to evaporate all of the xylene.

To assess the quality of the exposures and the degree to which the contrast curve was captured the sample is examined under an Olympus BX 60M optical microscope. The sample is studied to determine the number of exposures, which gives the minimum time required to create a partially polymerized exposure, and the minimum time for a fully polymerized exposure. The exposed areas as seen under an optical microscope are seen as a tan rectangle, which are darker with a greater thickness. At this point it is determined if a new sample must be run or if the current sample is of high enough quality to produce an accurate contrast curve.

3.3 Imagingof the Calix[6]arene exposures

To quantify the results of the exposures it is necessary to image the exposed regions using equipment that can accurately measure the step height of each exposure. There are several pieces of equipment capable of this, however an atomic force microscope (AFM) is the most accurate and easiest to use for this application. The AFM used was a Veeco Dimension 3100 Nanoscope IV, shown in figure 3.5.

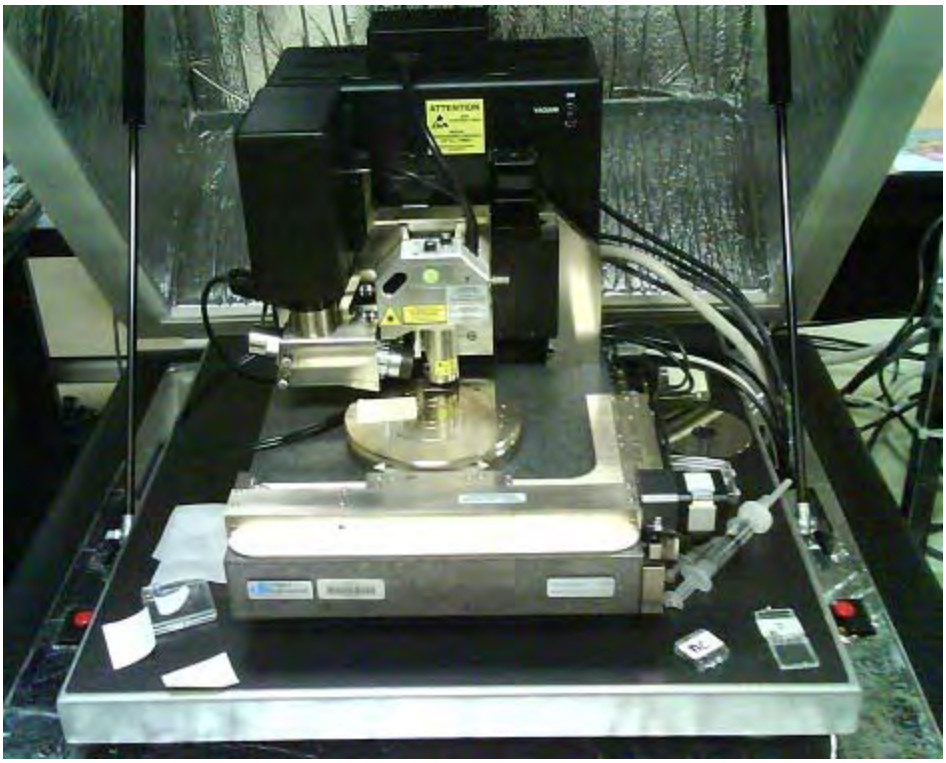

Figure 3.6: Veeco Dimension 3100 Nanoscope IV.

An AFM works by rastering a very small tip, normally etched silicon, across the surface of a sample. The tip is at the end of a cantilever, a small normally triangular arm that can flex to allow the tip to move to match the contours of the sample. On this AFM, the cantilever is mounted to a piezoelectric arm to scan the tip across the sample, in other AFMs the sample is mounted on the piezo and the tip is held static. A laser is reflected off of the cantilever onto a photodetector. The detector has four quadrants and is adjustable such that the laser is reflected onto the center of the four quadrants, as shown in Figure 3.7. As the tip travels over the sample it flexes the cantilever causing the reflected laser light to move across the detector's different quadrants. The AFM takes the signal from the four quadrants along with the position of the piezo to create a

topographic map of the sample. With a vertical resolution of less than 1nm the AFM is the best option available to analyze the exposed calix[6]arenes.

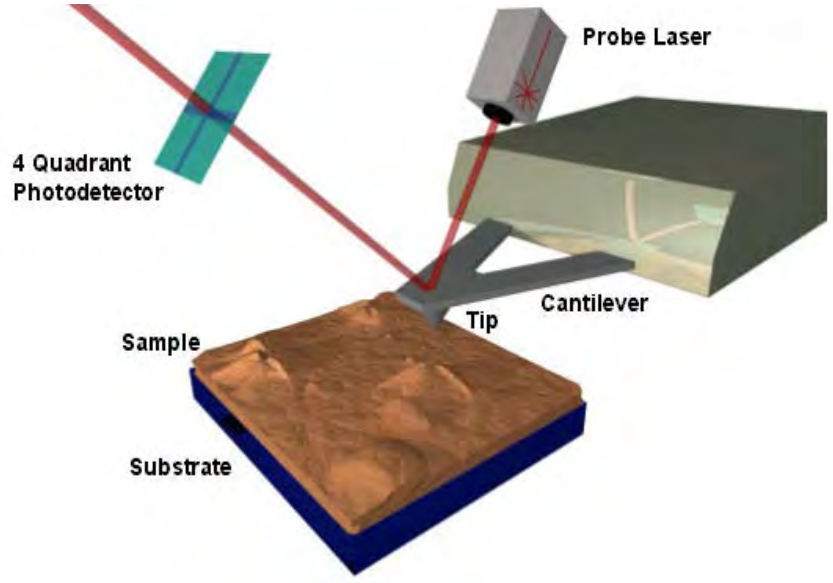

Figure 3.7: Basic Configuration for an Atomic Force Microscope.

The AFM is housed in a sound deadening hood, to prevent ambient noise from affecting the tip. Supporting the instrument is a large slab of granite which is on an air table for further vibration isolation. After the AFM is powered on the sample is placed on the sample stage using a vacuum chuck to hold the sample in place for scanning. The tip should be changed at this point to ensure scans of high quality. Tip life tends to average around 50 images, enough roughly for one sample. This was extended from fewer than 10 by baking the samples after the development process; it is believed that xylene residue was coating the tip causing premature failure. After the tip is replaced, requiring realignment of both the laser to the tip and the detector to the laser, the sample may be scanned. The onboard optical microscope allows for easy location of the samples for imaging,

the optical microscope is capable of imaging using magnifications of 20x to 200x. The samples were imaged from last to first in order to properly number them, and were imaged using a 50μm scan size.

To analyze the data taken from the AFM the Veeco Nanoscope analysis software was used. For each scan the step height of the exposure was measured three times to reduce possible errors from piezo drift or other scan anomalies. Once measured, the data was collated and formatted in Microsoft Excel.

CHAPTER 4

Results

Thickness data were collected using the Gaertner L117 null ellipsometer and was analyzed using the Film Wizard program. The thicknesses of the films varied significantly, up to 22.50nm, but averaged 25.26 ± 6.15nm. The variations are attributed in part to varying concentrations of the respective calix[6]arene solutions. Some of the containers for the calix[6]arenes did not seal properly causing the concentration of those solutions to increase as the chlorobenzene evaporated. The increased percent weight of the calix[6]arene solutions should have no appreciable effect on the films except to increase film thickness. It is also possible that variations in the application of the calix[6]arene during the spinning process could have caused variations in film thickness. An interesting result from the ellipsometric analysis is that the index of refraction (n) of the calix[6]arene does not appear to be dependent upon the functionalization. The average index of refraction is 1.55 ± 5.66E-3. The only sample that deviated significantly was the 0 cone sample, with an index of refection of 1.56, which may be due to its increased film thickness. The thickness of the native silicon dioxide (SiO_2) layer was also consistent, having an average thickness of 2.56 ± 0.48nm. Parameters

of SiO_2, such as the index of refraction, are well known and are included in the Film Wizard program. Because of this the index of refraction of the SiO_2 layer was not a calculated parameter, which is why it is not shown in the table below. No testing was done to see how the spin rate affects film thickness, however given the equation for centripetal force it is expected to have a large role.

$$F_{centripetal} = mr\omega^2 \qquad (4.1)$$

Where F is the centripetal force, m is the mass, r is the radius and ω is the angular velocity.

When an exposed sample was first developed, a deliberate attempt to underdevelop the sample was made, since the proper development time was not known and in this instance an underdeveloped film is of greater use than an overdeveloped film as the sample can be further developed to approach the correct time. As the proper development times were discovered it was seen that the higher functionalized groups were more resistant to solvents and required a longer development time to become fully developed. After several trials it was found that the calix[6]arenes functionalized with zero or two allyl groups required roughly eight seconds to fully develop, calix[6]arenes functionalized by four allyl groups would take roughly ten seconds, calix[6]arenes functionalized by six allyl groups would take roughly twelve seconds, and those with eight allyl groups would take roughly fifteen seconds. The functionalization appears to be tied to the solubility of both the polymerized calix[6]arene and the calix[6]arene monomers, with the fully functionalized groups taking close to twice as long to develop as the non-functionalized groups.

Table 4.1: Ellipsometry Data and Results.

Sample		P1	P2	Delta	A1	A1	Psi	angle	n	Thickness
0 Cone										
	SiO_2	50.4	140	169.6	11.1	169.3	10.9	70		3.4624nm
	Calix	87	177.7	95.3	22.9	159.7	21.6	70	1.561	39.9345nm
2 Cone										
	SiO_2	47.9	138.5	173.6	10.9	169.4	10.75	70		1.9969nm
	Calix	78.2	167.9	113.9	17.9	164.1	16.9	70	1.544	27.1565nm
4 Cone										
	SiO_2	49.1	138.4	172.5	11.6	168.8	11.4	70		2.5642nm
	Calix	75.1	162.8	122.1	15.3	166.2	14.55	70	1.543	19.9914nm
6 Cone										
	SiO_2	48.7	137.7	173.6	11.9	168.8	11.55	70		2.1855nm
	Calix	74.4	165.5	120.1	16.8	165	15.9	70	1.543	23.4279nm
8 Cone										
	SiO_2	49	138.1	172.9	11	169.2	10.9	70		2.2829nm
	Calix	78.2	168.9	112.9	18.2	164.2	17	70	1.545	26.861nm
0 Alt										
	SiO_2	48.9	138.5	172.6	10.9	168.9	11	70		2.4174nm
	Calix	78.7	168.9	112.4	17.9	164	16.95	70	1.545	27.1718nm
2 Alt										
	SiO_2	48	132.5	179.5	11.9	169.3	11.3	70		3.2364nm
	Calix	68.4	160.2	131.4	8.8	167.7	10.55	70	1.545	17.4371nm
4 Alt										
	SiO_2	50.1	138.1	171.8	11.8	169.5	11.15	70		2.7517nm
	Calix	73.5	164	122.5	15.8	165.9	14.95	70	1.540	20.5062nm
8 Alt										
	SiO_2	48.1	138.5	173.4	11.3	169.4	10.95	70		2.1157nm
	Calix	76.2	167.1	116.7	17.1	164.8	16.15	70	1.544	24.8129nm

There was no apparent difference in solubility between the two tested conformations; however, it would be necessary to perform an in depth study on the etch rates to determine any variations, as the development times above are rough approximations.

Data collected from the AFM were collated in Microsoft Excel, sorting the data by sample and exposure time with the recorded beam current. To this is added the exposure area. This is done as to create a graph that plots percent thickness after development versus electron dose measured in coulombs per square centimeter ($^{C}/_{cm^2}$), the latter of which is calculated using the following.

$$^{C}/_{cm^2} = ^{It}/_{A} \qquad (4.2)$$

Here C is coulombs, cm^2 is centimeters squared, I is the beam current, t is the exposure time and A is the exposure area in square centimeters. This is referred to as the dose and allows for the most accurate comparison between the different calix[6]arene films. One might ask why film thickness was not added to the equation. Despite large variances in thickness between films, the thickest film being 129% thicker than the thinnest film, in general it is not necessary to account for film thickness. At 20kV accelerating voltage it is believed that the incident electrons travel through the calix[6]arene film, breaking the carbon double bonds they come in contact with, and the initial energy of 20keV should be sufficient to break any number of the carbon double bonds that the electrons may encounter as they travel through the film.

Initial results were positive with the exposed regions visible under an optical microscope after development, giving a proof of concept, shown in Figure 4.1. It was also shown that exposures of differing times would produce regions of

differing post-development thickness, the longer exposures producing thicker regions.

Initial AFM scans were very hard on tips, which needed replacement about every 10 scans. The development procedure was modified by adding a one minute bake at 105°C to remove any excess xylene from the sample surface. It was also seen that some of the developed calix[6]arene would come back in contact with the substrate and adhere to the surface, possibly because of surface tension. This caused a “pimple” effect over the surface of the sample, which was solved by stirring the sample slightly more vigorously at the end of the xylene development.

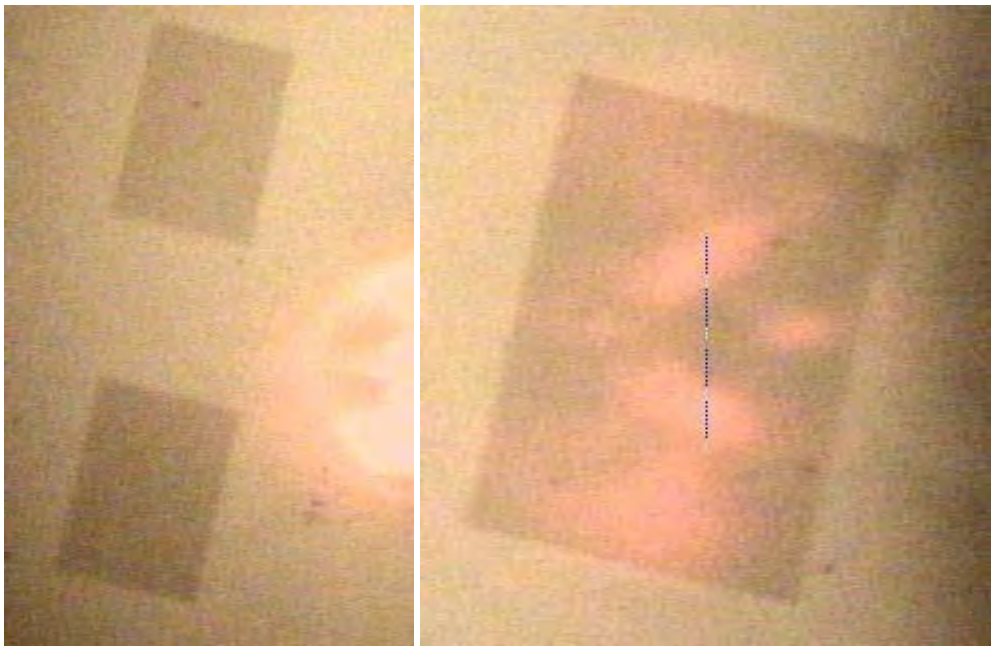

Figure 4.1: Calix[6]arene exposures after development. Captured by the Veeco AFM optical camera.

Of interest is the way in which the calix[6]arenes polymerized and developed. Some AFM images caught a glimpse of this as in figure 4.2. It is

believed that the lighter region is a large section of exposed and polymerized calix[6]arene that was separated during development and then landed over a portion of the scanned area. This gives some insight into how the calix[6]arene may polymerized. As expected the calix[6]arenes seem to be exposed evenly throughout, possibly polymerizing in distinct but initially separate layers. The layers, likely divided by a layer of calix[6]arenes that have not been fully exposed or polymerized, might become separated during the development process allowing the upper layer or layers to float in the developer and land elsewhere on the substrate. It is also noteworthy that this effect seems to be limited to calix[6]arenes functionalized with six or eight allyl groups, again suggesting that the higher functionalized groups may be more resistant to solvents.

Contrast curves were plotted in logarithmic form, and for convenience the units chosen for the dose were micro coulombs per square centimeter ($\mu C/cm^2$).

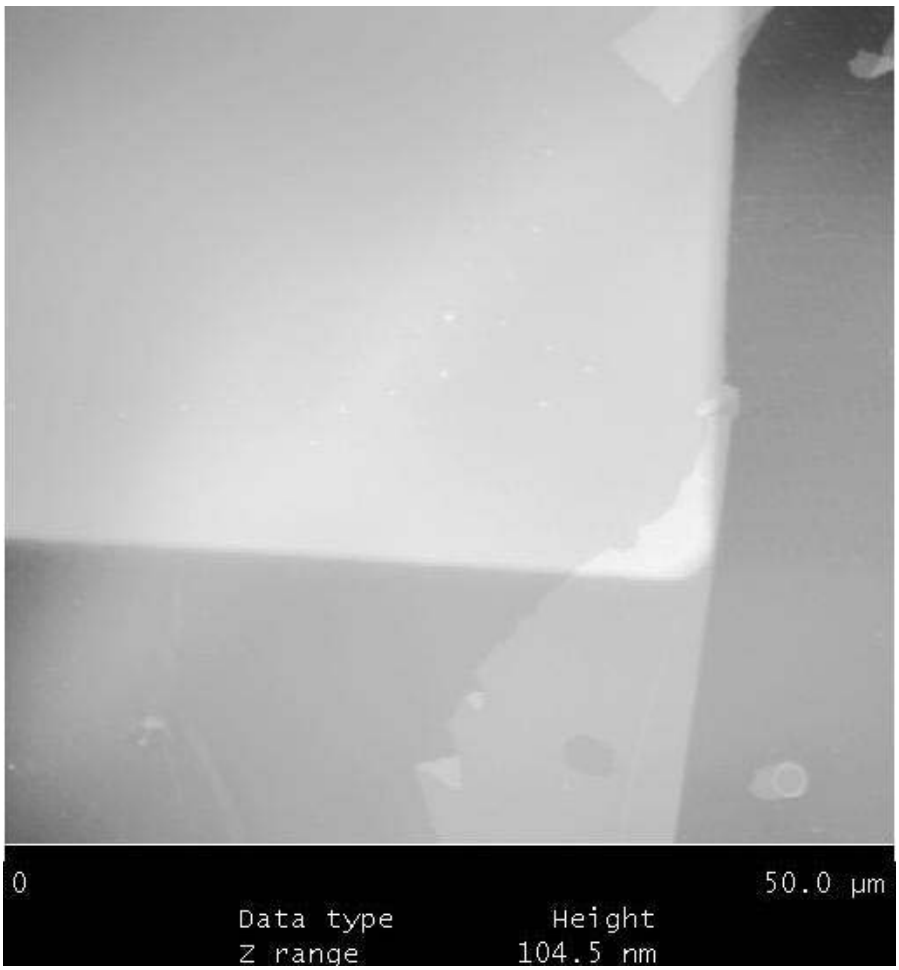

Figure 4.2: AFM image of an exposure of an 8 Cone film. The Larger rectangle is an exposed region of the calix[6]arene film. The lighter regions are possibly pieces of thin layers of exposed regions that were separated during the development process and landed back on the substrate.

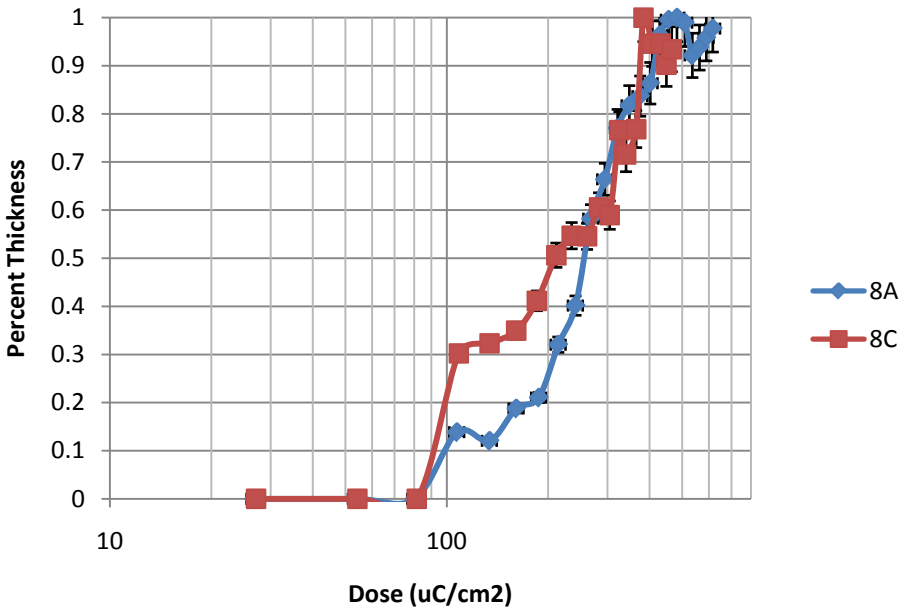

Figure 4.3: Thickness versus Dose of calix[6]arenes with eight allyl groups.

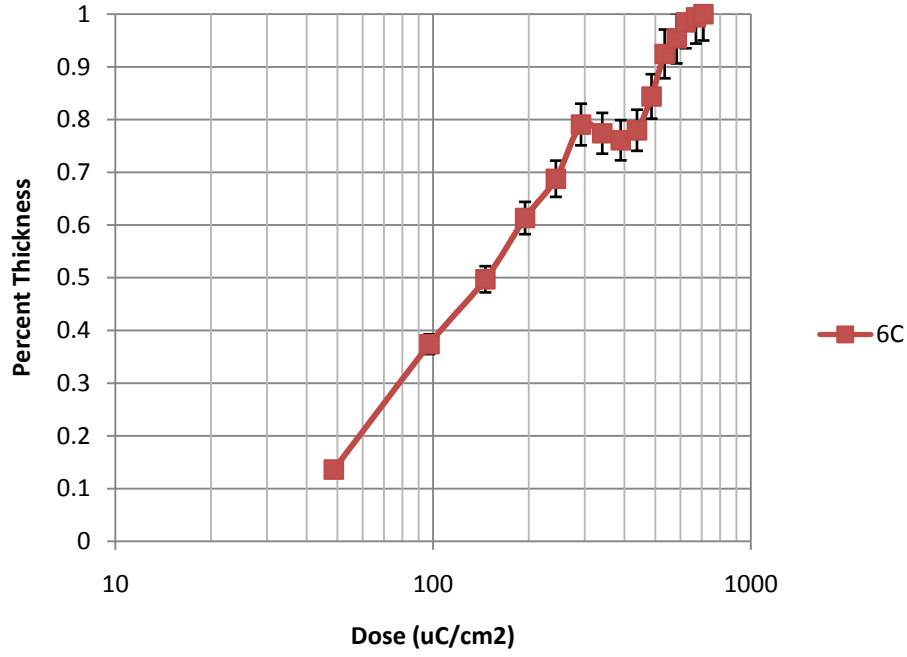

Figure 4.4: Thickness versus Dose of calix[6]arenes with six allyl groups.

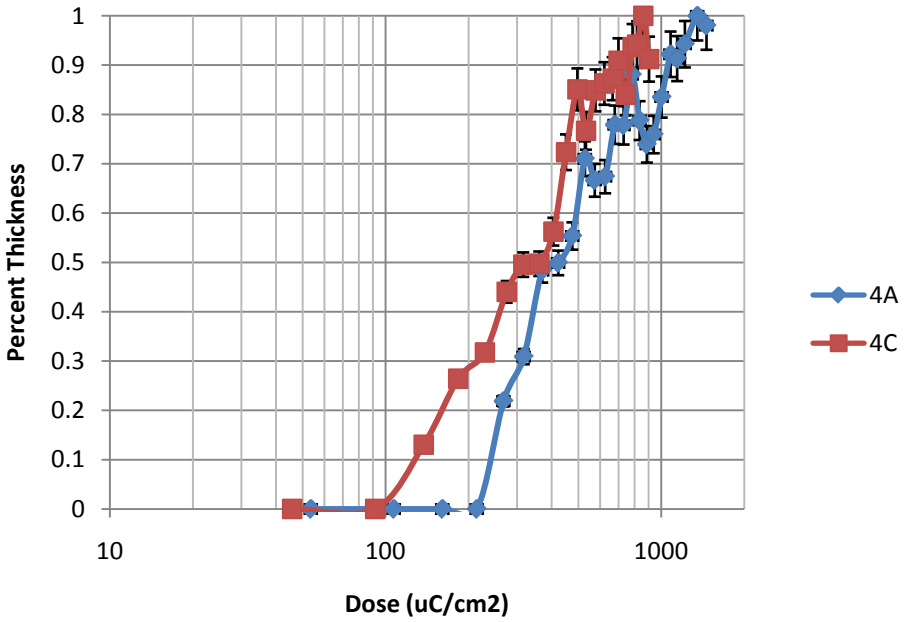

Figure 4.5: Thickness versus Dose of calix[6]arenes with four allyl groups.

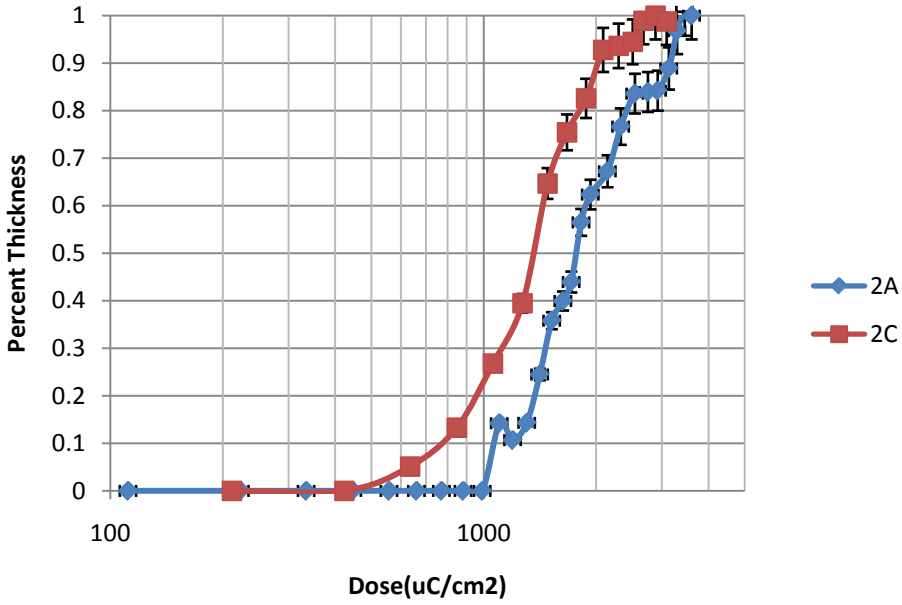

Figure 4.6: Thickness versus Dose of calix[6]arenes with two allyl groups.

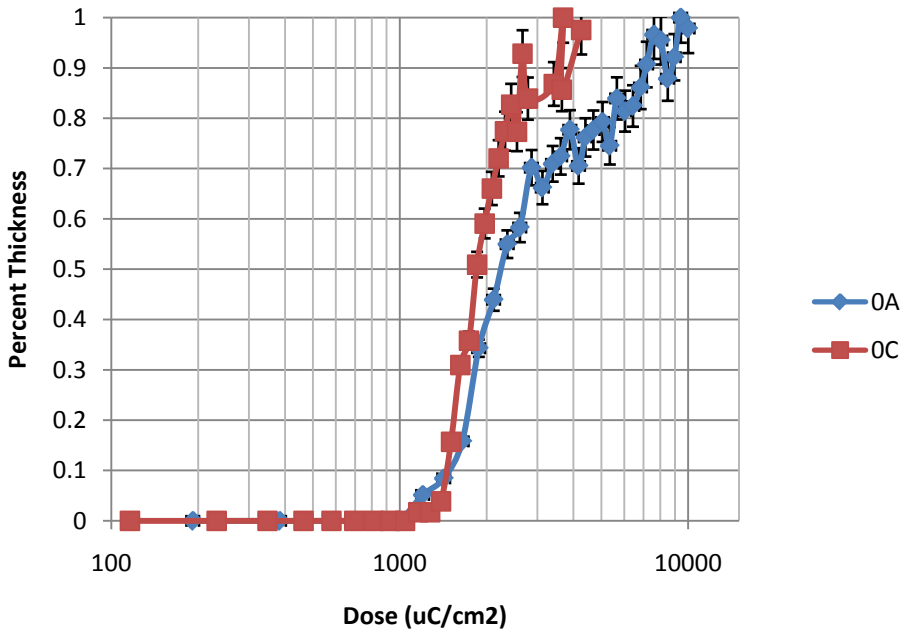

Figure 4.7: Thickness versus Dose of calix[6]arenes with no allyl groups.

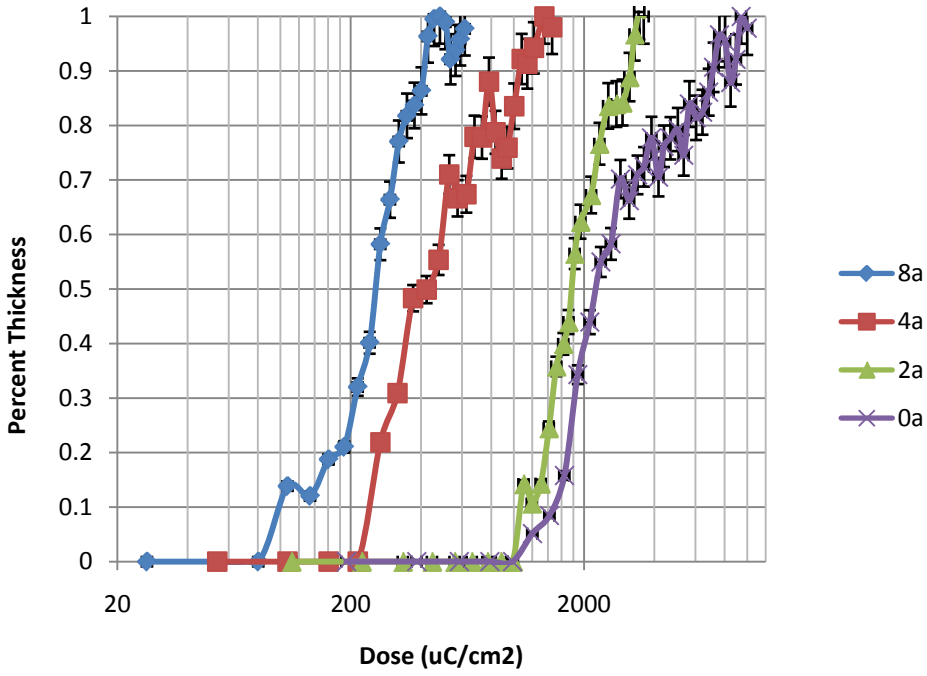

Figure 4.8: Thickness versus Dose of the 1-2-3-alt calix[6]arenes.

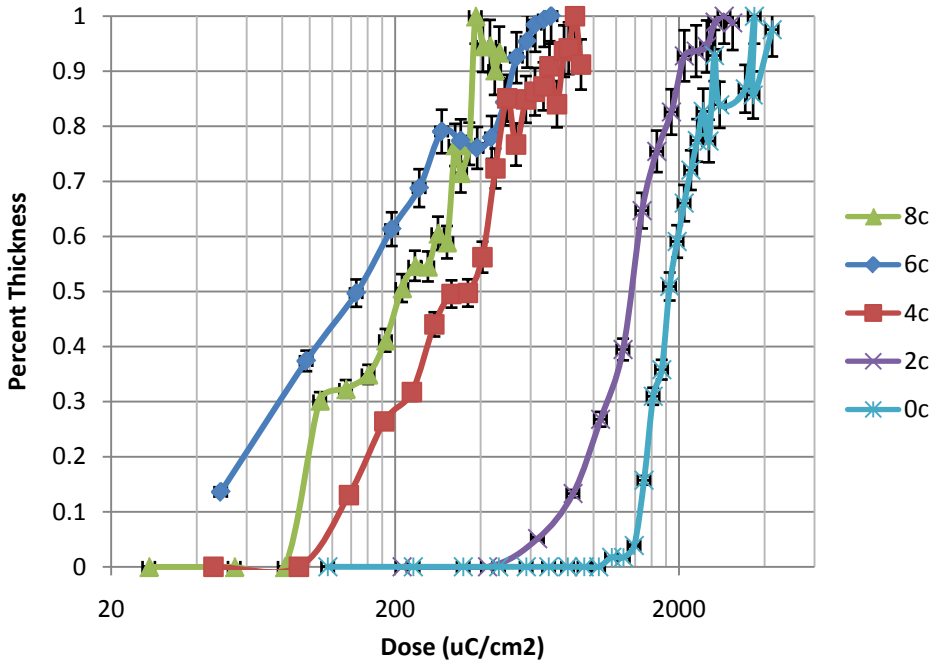

Figure 4.9: Thickness versus Dose of the cone calix[6]arene.

An observant reader will have noticed that there is no 6 alt curve as it was not available at the time of writing. The respectively functionalized calix[6]arenes of the different conformations have very similar contrast curves and sensitivities, though in most cases the cone conformation has a slight advantage in sensitivity. As expected an increase in functionalization with allyl groups gave an increase in sensitivity to electron exposure, as shown in figure 4.11. Interestingly the functionalized groups tended to group in sensitivity. The groups functionalized with zero and two allyl groups have similar sensitivities, as do the groups functionalized with four, six for the cone conformation, and eight allyl groups. However there is a large gap between the two, which suggests that there is a minimum number of allyl groups needed to greatly affect the sensitivity of the base calix[6]arene. The large sensitivity difference between the 0 cone and 0 alt

is also interesting. Comparing the two shows that conformation may have a substantial affect on sensitivity. The functionalized groups have much closer sensitivities, suggesting that any contribution to the sensitivity by the conformation is masked by the addition of allyl groups which appear to have a much greater impact. It would also suggest that the conformation only has a minor impact on the way in which allyl groups create intermolecular bonds.

Contrast is taken to be the slope of the log plot, which is why the curves above are plotted in log form. The plot is given a best fit line through the linear portion of the contrast curve, as shown in figure 4.10. Where this best fit line intersects the X-axis at zero thickness is taken to be the gel dose (D_g), or the minimum dose to gain a response from the calix[6]arene. The point at which the line intersects with the full normalized thickness (1 on the Y-axis) is taken to be that dose required for full exposure, referred to as the insolubilization dose (D_i), also used in figure 4.10. The slope is taken as the following.

$$Contrast\ (\gamma) = \frac{1}{Log_{10}(D_i) - Log_{10}(D_g)} = \frac{1}{Log_{10}(\frac{D_i}{D_g})} \qquad (4.3)$$

In this expression γ is the contrast, and the log of D_g and D_i are taken to give the logarithmic slope. It should also be noted that D_i is also the sensitivity, as used in figure 4.11.

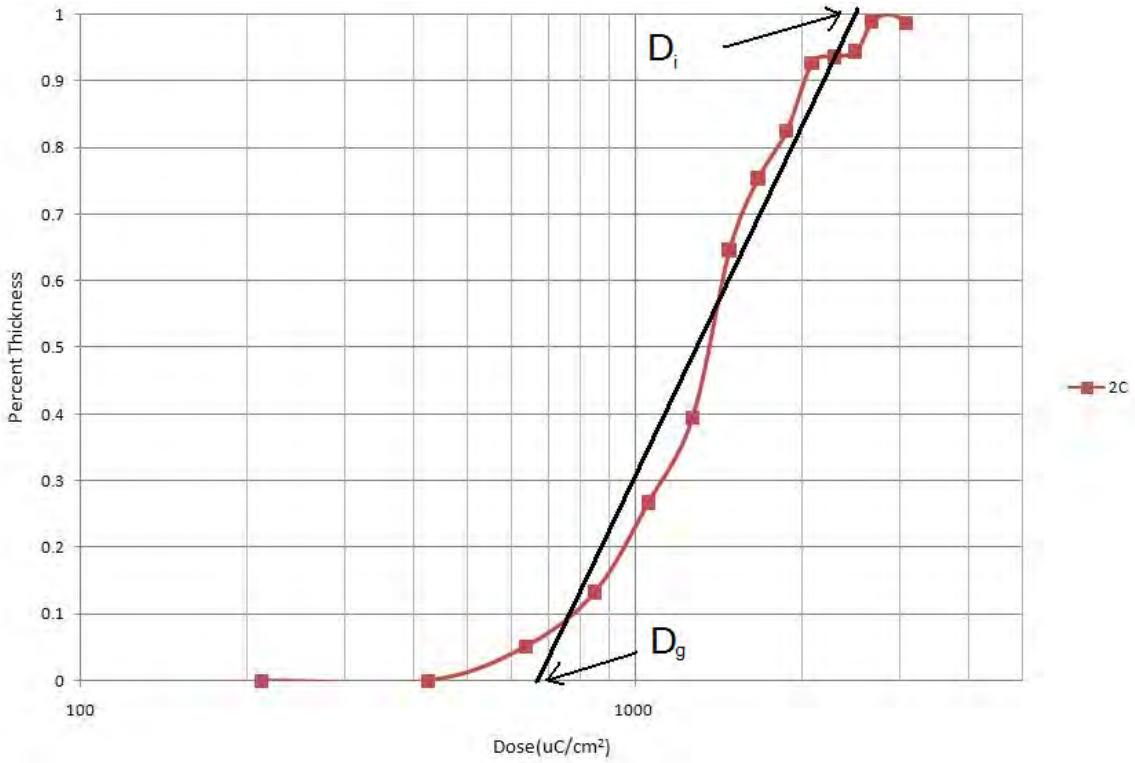

Figure 4.10: Contrast best fit line for 2 Cone.

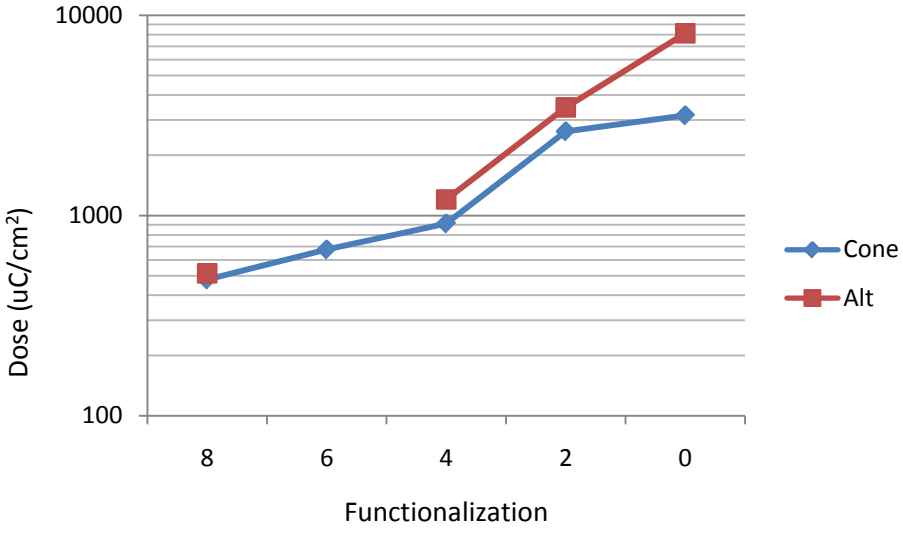

Figure 4.11: Sensitivity for the Cone and 1-2-3-Alt calix[6]arenes.

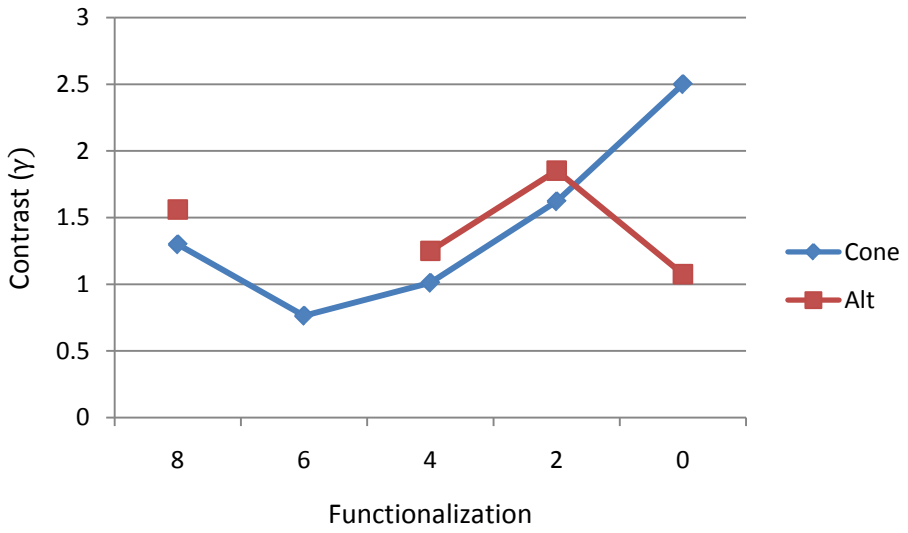

Figure 4.12: Contrast versus Functionalization.

It does not appear that the contrast is dependent on functionalization in quite the manner expected. When considering the cone isomer it is only when functionalized with eight allyl groups that the calix[6]arene deviates from the expectation that a higher sensitivity will result in a lower contrast. With the alt isomer, however, the non-functionalized calix[6]arene is also well off from expectations. Without the 6 alt calix[6]arene it is difficult to discern a pattern for the 1-2-3-alternate group, or if the two conformations follow the same curve. The cone and alt isomers do match well when considering those functionalized by eight, four and two allyl groups, with the alt isomer showing a slightly better contrast. This corresponds with cone isomer having an increased sensitivity, again pointing to a possible inverse relationship between sensitivity and contrast. The large difference between the 0 cone and 0 alt samples suggest that conformation plays a large role in the contrast, but that any functionalization by allyl groups masks the affect to a large degree.

Table 4.2: Table of calix[6]arene contrast and sensitivity.

Sample	D_g ($\mu C/cm^2$)	D_i ($\mu C/cm^2$)	Contrast(γ)	Sensitivity ($\mu C/cm^2$)	Development Time
8 Alt	117.4898	514.0437	1.56	514.0	15 Seconds
8 Cone	81.28305	478.6301	1.30	478.6	15 Seconds
6 Cone	33.11311	676.083	0.76	676.1	12 Seconds
4 Alt	190.5461	1202.264	1.25	1202.3	10 Seconds
4 Cone	93.32543	912.0108	1.01	912.0	10 Seconds
2 Alt	1000	3467.369	1.85	3467.4	8 Seconds
2 Cone	676.083	2630.268	1.69	2630.3	8 Seconds
0 Alt	954.9926	8128.305	1.08	8128.3	8 Seconds
0 Cone	1258.925	3162.278	2.5	3162.3	8 Seconds

CHAPTER 5

Conclusion

5.1 Summary

All available compounds performed well as a negative electron beam resist. The compounds proved capable of long term storage in the liquid form, given properly sealed containers. Once deposited on a wafer the unexposed films were capable of sitting for long periods of time with no signs of film degradation or decreased capabilities as a resist. Films that were several days old were tested against films that were 6 months old with no noticeable difference in performance.

Substrate characteristics were uniform with an average silicon dioxide film thickness of 2.56 ± 0.48nm. Because of containers that did not properly seal and possible variations during the spin application the calix[6]arene film thicknesses were more inconsistent than expected. The films were deposited by spinning them on at 3000 rpm for 30 seconds, giving an average film thickness of 25.26 ± 6.15nm. Changing the rate that the film is spun on can change this significantly, as can increasing the concentration of the solutions. Despite possible variations in concentration and the variations in film thickness, the index of refraction of the films was very uniform averaging 1.55 ± 5.66E-3.

A JEOL JSM-6400F high resolution field emission SEM was used to expose the samples. This SEM is capable of producing roughly 0.5-1nA of beam current. Most samples were fully exposed at 1k magnification by a dose of 500 to 1200 $\mu C/cm^2$, with the exception of the calix[6]arenes with either zero or two allyl groups which required 2k magnification and where fully exposed by a dose ranging from 2500 $\mu C/cm^2$ to just over 8000 $\mu C/cm^2$.

AFM imaging clearly showed exposed regions and facilitated the creation of accurate contrast curves. The sensitivity of the calix[6]arenes varied with functionalization and was less dependent on the conformation of the calix[6]arene. Results did show that the 1-2-3-alternate conformation was slightly less sensitive than the cone conformation, but with a slightly higher contrast when functionalized by two, four or eight allyl groups. It was found that the higher functionalized calix[6]arenes were much more sensitive than those with lower functionalization. Contrast did vary between the various conformations and with the level of functionalization, but this behavior is not yet understood.

In comparison to PMMA, calix[6]arenes functionalized with eight allyl groups are slightly less sensitive. PMMA has a sensitivity of around $100\mu C/cm^2$ where the calix[6]arenes with eight allyl have a sensitivity of roughly $500\mu C/cm^2$.[5] This also compares well with literature on the calix[4]arene, which have shown sensitivities on the order of $1mC/cm^2$.

5.2 Future Work

While the calix[6]arene will polymerize when exposed to an electron beam, and do so with a relatively high sensitivity and contrast, there are many factors

left to consider before choosing to use it as a resist. In practice it will be necessary to produce thicker films, and as such spin curves would be very useful to ascertain the thickest possible film. It will also be important to understand how the exposed and polymerized film reacts to different solvents. A study of etch rates with different solvents typically used during common semiconductor processes is also of high importance. Plasma etch rate study would also be useful. Understanding the relationship between acceleration voltage and exposure time is another aspect of key importance. Creating a table relating the sensitivity of the calix[6]arenes to the thickness of the calix[6]arene film and the accelerating voltage should be a high priority in future research.

A resolution study is possibly of the highest importance. Resolution defines the smallest features size it is possible to create with a particular resist, and in this case is likely defined by the size of the calix[6]arene. This will require an electron source with extremely high resolution, as it will need to be smaller than the resolution of the calix[6]arene resist. Previous studies have found calixarenes to have a resolution of roughly 10nm, so an SEM should be capable of performing the task if equipped with the proper writing equipment. [9]

Bibliography

[1] Kuller, A.; Eck, W.; Stadler, V.; Geyer, W.; Golzhauser, A., "Nanostructuring of Silicon by Electron-Beam Lithography of Self-Assembled Hydroxybiphenyl Monolayers", *J. Appl. Phys.,* 2003, 82(21), 3776.

[2]Kendall, Russel C., *Charaterization of Differentally Functionalized, Conformationally Locked Calix[6]arenes as Negative Electron-Beam Lithography Resist.* Texas State University-San Marcos, May 2007

[3]Wikepedia, *Moore's Law, http://en.wikipedia.org/wiki/Moore's_Law*

[4]Thompson, L. F., *in* Thompson, L. F..; WIllson, C. G.;Bowden, M. J. Introduction to Microlithography, Second Edition, American Chemical Society: Washington, D. C., 1994.

[5] Gutsche, C. D. Calixarenes In Monographs in Supramolecular Chemistry, ed. Stoddart, J. F. The Royal Society of Chemistry: Cambridge, England, 1989.

[6] Gutsche, C. D. Calixarenes Revisited In Monographs in Supramolecular Chemistry, ed. Stoddart, J. F. The Royal Society of Chemistry: Cambridge, England, 1998.

[7] Mandolini, L.; Ungaro, R. Calixarenes In Action, ed. Mandolini, L.; Ungaro, R. Imperial College Press: London, 2000.

[8] Arduini, A.; Casnati, A. "Calixarenes" in Macrocyclic Synthesis: a Practical Approach, ed. Parker, D. Oxford University Press: Oxford, 1996.

[9] Fujita,J.; Ohnishi, Y.; Ochiai, Y.; Matsui, S. "Ultrahigh resolution of calixarene resist in electron beam lithography" *Appl. Phys. Lett.*, 1996, *68(9),* 1297-1299.

VITA

Daniel Matthew Ralls was born in Houston, Texas, on December 26, 1980, the son of Kay Hemphill Ralls and Walter Matthew Ralls. Graduating in 2000 from Memorial Senior High School, Houston, Texas, he enrolled at Houston Community College. In 2001 he transferred to the University of Texas at San Antonio, and in 2002 he transferred to Texas State University-San Marcos. He earned a degree of Bachelor of Science in Physics from Texas State in August of 2006. In the same month he enrolled in the University of Oklahoma. In August, 2007, he enrolled in the Texas State University Graduate College, earning a degree of Masters of Science in Physics on December 20, 2008.

This thesis was written by Daniel Matthew Ralls.